Biophysical Chemistry 197 (2015) 1–9

Contents lists available at ScienceDirect

Biophysical Chemistry

journal homepage: http://www.elsevier.com/locate/biophyschem

Biophysical processes affecting DOM dynamics at the Arno river mouth (Tyrrhenian Sea)

S. Retelletti Brogi *, M. Gonnelli, S. Vestri, C. Santinelli

Istituto di Biofisica, CNR, Pisa, Italy

HIGHLIGHTS

- A biophysical approach to the study of marine carbon cycle
- Biochemical transformation of dissolved organic matter in a coastal area
- Study of chromophoric dissolved organic matter through absorption and fluorescence spectroscopy

GRAPHICAL ABSTRACT

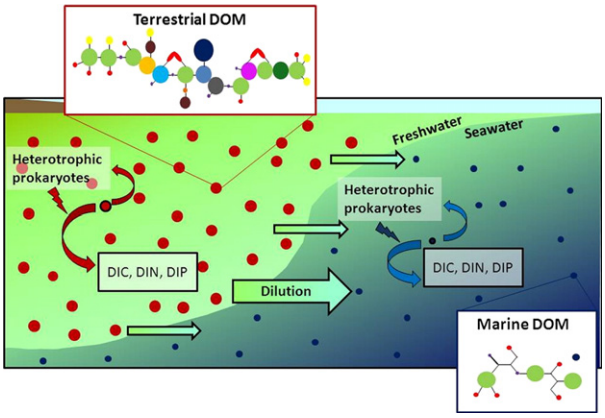

ARTICLE INFO

Article history:
Received 1 September 2014
Received in revised form 13 October 2014
Accepted 27 October 2014
Available online 4 November 2014

Keywords:
CDOM
Fluorescence EEM
Absorption spectroscopy
River
Mineralization rate
DOC

ABSTRACT

Dissolved organic carbon (DOC) and optical properties (absorption and fluorescence) of chromophoric dissolved organic matter (CDOM) were measured in October 2012, at the Arno river mouth and in a coastal station close to it. The data reported indicates that the Arno river represents an important source of DOC and CDOM to this coastal area, with a total DOC flux of $11.23–12.04 \cdot 10^9$ g C·y^{-1}.

Moving from the river to the sea, CDOM absorption and fluorescence decreased, while the spectral slope increased, suggesting a change in the molecular properties of CDOM.

Mineralization experiments were carried out in order to investigate the main processes of DOM removal and/or transformation in riverine and coastal water. DOC removal rates were 20 μM·month^{-1} in the river and 3 μM·month^{-1} in the seawater, while CDOM was released during the first 30 days and removed in the following 40 days.

1. Introduction

Dissolved organic matter (DOM) is a complex mixture of molecules, the majority not yet characterized at a molecular level. DOM is the main source of food for heterotrophic prokaryotes, representing a reservoir of energy for marine ecosystem. Depending on the bioavailability of its molecules, DOM has been divided into two different fractions, the labile fraction with a lifetime from few hours to days, and the recalcitrant fraction, which is more persistent and is divided into 4 other fractions: the semi-labile (lifetime ~1.5 years), the semi-refractory (lifetime ~20 years), the refractory (lifetime ~16,000 years) and the ultra-refractory (lifetime ~40,000 years) [1].

* Corresponding author.
E-mail address: simona.retelletti@pi.ibf.cnr.it (S. Retelletti Brogi).

http://dx.doi.org/10.1016/j.bpc.2014.10.004
0301-4622/

DOM in the oceans contains 662 Pg C, representing 93% of the active carbon reservoir on the Earth [1]. It plays an important role in the global carbon cycle with particular regard to CO_2 sequestration from the atmosphere [2].

Coastal areas represent only 0.5% of the ocean surface but they are characterized by high carbon fluxes, due to terrestrial inputs. The global input of total organic carbon (TOC) into the oceans from freshwaters has been estimated to be ~0.45 $Pg \cdot y^{-1}$ [3], and it accounts for 0.024% of the oceanic TOC pool [4]. In the Mediterranean Sea, the river input may represent 0.08–0.3% of the TOC pool [5]. CO_2 exchange between ocean surface and the atmosphere is very intense in coastal and estuarine areas, even if it is not clear if they act as a source or a sink of C. It has been estimated that in coastal areas, heterotrophic organisms can respire ~50% of terrestrial carbon annually [6]. Borges et al. [7] estimated that the global coastal systems may release ~0.4 Pg $C \cdot y^{-1}$, balancing the 0.45 Pg C trapped annually in the global oceans. Despite their importance, coastal and estuarine areas were ignored for a long period in the global carbon budget.

The key role of coastal areas in the global carbon cycle is mainly linked to the biophysical processes affecting particulate (POM) and dissolved organic matter (DOM) dynamics. A rapid decrease in DOM concentration has been observed moving from the rivers to the open ocean, together with a change in chromophoric DOM (CDOM) optical properties. Different biological and physical processes can explain this observation: (1) dilution, determining a conservative behavior of terrigenous DOM [8]; (2) flocculation phenomena, induced by the change in physical conditions, leading to the sequestration of DOM in the sediments [9]; (3) photodegradation [10] and (4) microbial removal and transformation [11]. It has recently been demonstrated that coastal microbial communities control the flow of dissolved organic carbon (DOC) from terrestrial sources and regulate the release of inorganic carbon into the atmosphere [12]. The interaction between physical and biogeochemical processes results in temporally and spatially variable dynamics in ocean margins, making an estimation of the carbon fluxes difficult [13].

DOC and optical properties (absorption and fluorescence) of CDOM have been used to study the dynamics of DOM in coastal areas influenced by river inputs [5,13–22]. Studies in the Mediterranean Sea, focus on the Po [16,22] and the Rhone river [5,17,19], the main fresh water inputs to the Mediterranean Sea after the building of the Aswan Dam, and the Arno river [14,20,21].

DOC shows similar concentration in the Rhone (134-217 μM) and Po river (175 μM) (Table 1), even if their characteristics are different in terms of population density in the watershed, solid transport and discharge [22]. It is worth noting that in the Arno river the DOC concentration is markedly higher (322-402 μM) than that reported for the other Mediterranean rivers (Table 1, [23]). As a consequence, it could play an important and overlooked role in the Mediterranean Sea carbon budget, though its discharge is low. A conservative behavior was observed for both DOC and humic-like CDOM [14,16,20] at the mouth of Po and Arno river. In contrast, a non-conservative behavior was recently reported for both humic-like and protein-like CDOM at the mouth of the Arno and Rhone rivers [17,21]. This finding was explained by physical and biological processes (i.e. photobleaching, production and/or removal by both phytoplankton and heterotrophic prokaryotes) other than dilution.

The main goal of this study is to investigate the role of biophysical processes in DOM removal and/or transformation in a coastal system, by using a spectroscopic approach. A comparison of DOC concentration and CDOM absorption and fluorescence in the Arno river and in the coastal area, close to the river mouth, is reported together with a first estimate of the removal rates for riverine and marine DOC in this area.

2. Methods

2.1. Study area and sample collection

This study was carried out at the mouth of the Arno river (Pisa, Italy) (Fig. 1). The Arno river is one of the biggest rivers flowing into the Tyrrhenian Sea, it has a length of 241 km, a drainage basin area of $8.2 \cdot 10^3$ km^2 and an average discharge of 2.6 $km^3 \cdot y^{-1}$. During its route, the river flows through two big cities (Florence and Pisa) as well as industrial and agricultural areas (e.g. the tannery industry in Santa Croce sull'Arno), as a consequence the river is enriched by organic and anthropogenic pollutants.

Surface water was collected in 500 ml dark glass bottle at the mouth of the river and in the sea on October 10th 2012 (Fig. 1). The bottles were preconditioned with seawater and rinsed three times with the sample before filling. Samples for DOC and CDOM were immediately filtered through a sterile 0.2 μm nylon filter and stored in the dark at 4 °C until analysis.

Salinity and temperature were measured by using a portable Hanna 9033 conductivity instrument.

Data of river discharge are from the Regional Hydrological Service of Tuscany dataset (www.sir.toscana.it). A satellite map of chlorophyll-a distribution in this area was obtained from MODIS-Aqua and elaborated with regional algorithm MedOC3 [24]. The best coverage, in terms of clear sky, occurred on October 9th. The map was kindly provided by Dr. Gianluca Volpe (CNR — ISAC).

2.2. DOC measurements

DOC measurements were carried out by using a Shimadzu Total Organic Carbon analyzer (TOC-Vcsn), by high temperature catalytic oxidation. Samples were acidified with HCl 2N and sparged for 3 min with CO_2-free pure air in order to remove inorganic carbon. From 3 to 5 replicate injections were performed until the analytical precision was lower than 1% (±1 μM). A five point calibration curve was done by injecting standard solutions of potassium hydrogen phthalate in the concentration range between 20 and 350 μM. At the beginning and end of each analytical day, the system blank was measured using Milli-Q water and the reliability of measurements was checked by comparison of data with a DOC Consensus Reference Waters (CRM) [25] kindly provided by Prof. D.A. Hansell of the University of Miami.

Table 1
Discharge, drainage basin area [38], DOC concentrations and fluxes of the Arno river compared to the main Mediterranean rivers.

River	Length (km)	Discharge (km^3/y)	Drainage basin area (10^3 km^2)	DOC (μM)	DOC flux (10^9 g C/y)	Reference
Arno	241	2.6	8.2	365	11.38	This study
				402	12.54	[20]
				322	10.04	[14]
				352	10.98	[21]
Tevere	405	6.8	16.5	227	18.52	Santinelli, unpublished data 2010
Po	652	49.5	70.1	175 ± 50	103.95	[22]
Ebro	928	13.1	84.2	218	34.32	[15]
Rhone	812	54.3	95.6	217 ± 60	141.39	[5]
				113 ± 12	73.63	[17]
				134 ± 31	87.31	[19]

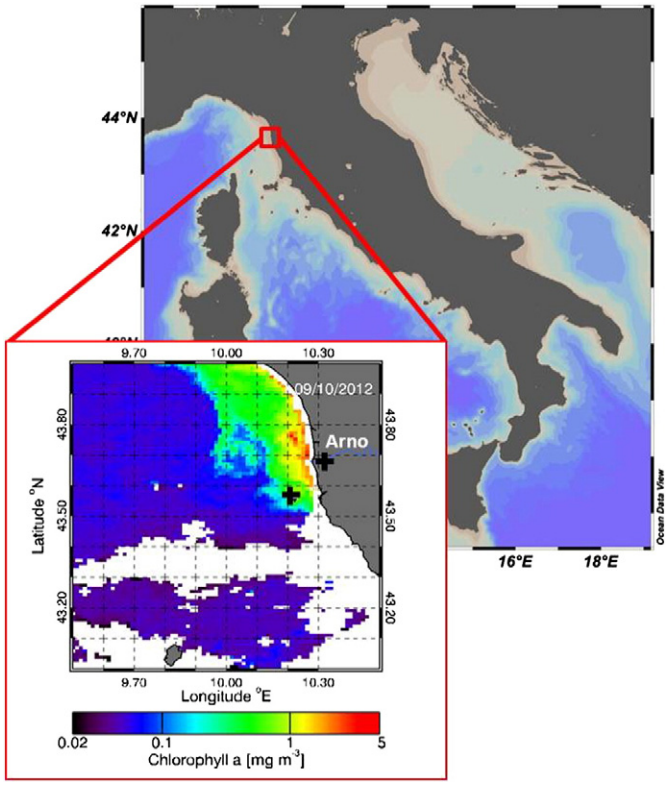

Fig. 1. Study area and sampling stations. In the zoom the chlorophyll satellite map of the area is reported.

DOC concentrations were calculated by Eq. (1) [26]:

$$\mathrm{DOC}\ (\mu\mathrm{M}) = \frac{(\text{sample area} - \text{system blank area})}{\text{slope of standard curve}}. \quad (1)$$

DOC was reported not to vary within 10 months in the storage conditions reported above [27].

2.3. CDOM optical properties

2.3.1. Absorption measurements

Absorption spectra were measured by a Jasco Mod-7850 spectrophotometer UV–visible, with a 10 cm quartz cuvette. Absorption spectra were registered between 230 and 700 nm every 0.5 nm. The absorption spectrum of Milli-Q water was subtracted from each sample spectrum [28].

Absorption coefficient was then calculated by Eq. (2):

$$a_{(\lambda)} = 2.303 \cdot A_{(\lambda)}/l \quad (2)$$

where A is the absorbance and l is the path length in meters. Absorption coefficient was calculated at 280 nm (a_{280}) and 355 nm (a_{355}), because at these wavelengths the excitation maximum is observed for protein-like and humic-like substances, respectively.

The spectral slope (S) of the absorption curve was calculated by using a non-linear fitting with the Eq. (3):

$$a_{(\lambda)} = a_{\lambda_0} \cdot e^{-S \cdot (\lambda - \lambda_0)} \quad (3)$$

where λ_0 is the first wavelength in the range and a_{λ_0} is the absorption coefficient at λ_0. S was calculated in the wavelength range 275–295 nm ($S_{275-295}$) because this range is characterized by the greatest variations [29] and $S_{275-295}$ can be related to the percentage of terrestrial DOC [13]. S was also calculated in the ranges 350–400 ($S_{350-400}$), 350–500 ($S_{350-500}$), and 270–Detection Limit (S_{270-DL}), in order to make a comparison with other studies carried out in coastal waters [17,20,29].

The same sample was analyzed 5 times during a period of 3 months, the repeatability test showed that the variation was less than $9 \cdot 10^{-5}$ m^{-1} for a_{355} and $6 \cdot 10^{-4}$ m^{-1} for a_{280}.

2.3.2. Fluorescence measurements

Tridimensional excitation–emission matrixes (EEMs) were recorded by the Aqualog fluorometer (Horiba) by using a $10 \cdot 10$ mm^2 quartz cuvette. The EEMs allow to distinguish between the fluorescence signals due to the diverse groups of chromophores. The Aqualog fluorometer uses a charge-coupled device (CCD) to reveal the signal, guaranteeing a high acquisition velocity and reduced photobleaching. The characteristics of the lamp improve the sensitivity of data acquisition at low excitation wavelengths (250–350 nm) allowing a better identification of the protein-like fluorescence. Excitation wavelength ranged between 250 and 450 nm at 5 nm increments, while emission was measured between 212 and 619 nm at 3 nm increments. Each EEM was corrected for the inner-filter effect [30], by using Eq. (4) [31]:

$$F_{corr} = F_{obs}\, 10^{\frac{A_{280}}{l}}. \quad (4)$$

EEMs were corrected for instrumental bias in excitation and emission and subtracted by the EEM of Milli-Q water (blank) measured in the same conditions before each sample. Rayleigh and Raman scatter peaks were removed by using the monotone cubic interpolation (shape-preserving) [32], since water subtraction did not completely remove their signals.

EEMs were normalized to the water Raman signal, dividing the fluorescence by the integrated Raman band of Milli-Q water (λ_{ex} = 350 nm, λ_{em} = 371–428 nm), measured the same day of the analysis. The fluorescence intensity is reported as equivalent water Raman Units (R.U.) [33].

In order to check the repeatability of our measurements the same sample was analyzed 5 times during a period of 3 months, the results showed that the variation was less than $5 \cdot 10^{-4}$ R.U.

2.4. Mineralization experiment

Mineralization experiments were carried out in a 500 ml dark glass bottle, by comparing DOC removal rates and changes in optical properties of CDOM in samples filtered through a sterile 0.2 μm nylon filter and stored in the dark at 4 °C (hereinafter control) and in samples filtered through a sterile 0.45 μm nylon filter and stored at 22 ± 2 °C (hereinafter mineralized samples). Three replicates were analyzed for both control and mineralized samples. The treatment for the control was chosen since no change in DOC concentration and CDOM optical properties was observed within 10 months in the storage conditions reported above (in the dark and at 4 °C) [27]. This procedure circumvented the need to employ chemicals to stop the microbial activity, since their interaction with DOM is not clear. The 0.45 μm pore size was chosen since it retains most of the heterotrophic prokaryotes inside the sample and it guarantees the removal of both autotrophic organisms and heterotrophic prokaryotic grazers [34]. As a consequence, we assume that the semi-labile DOM is removed by the heterotrophic prokaryotes occurring in the samples. Taking into consideration data from the literature for the Mediterranean Sea, the abundance of heterotrophic prokaryotes is ~$4.5 \cdot 10^6$ cells·ml^{-1} in the rivers (data from the Rhone river) [35] and ~$0.26–2 \cdot 10^6$ cells·ml^{-1} in the coastal areas [35,36]. The controlled temperature of 22 ± 2 °C was similar to the one measured in situ, in order to avoid thermal shock and a change in metabolic processes. DOC and CDOM optical properties were measured immediately after collection (t_0), after one month (t_1) and two months (t_2).

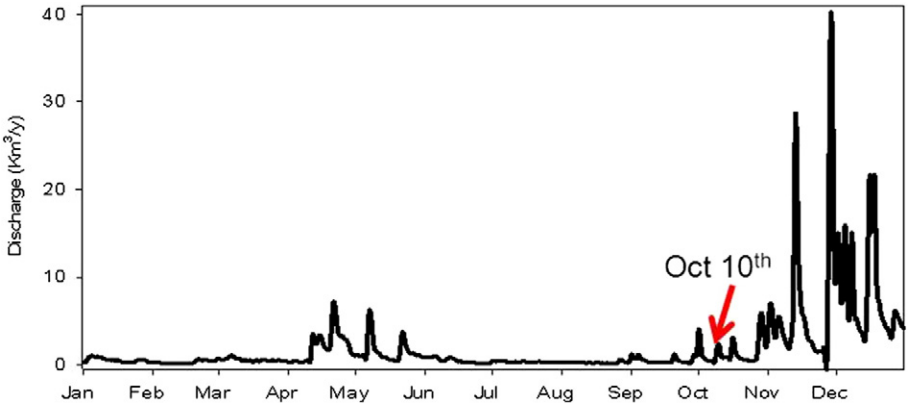

Fig. 2. Discharge of Arno river during 2012. Values of discharge were measured in a station located 37 km inside the river.

Before the analysis, 50 ml of each sample was filtered through a 0.2 μm nylon filter, under a laminar air flow hood.

2.5. Statistics

The Kruskal–Wallis test (R software) was used in order to test if the variations in DOC and optical properties of CDOM during the experiment were statistically significant. This test was chosen since it is a non-parametric test and does not need any distributional assumption [37]. Differences were considered significant for $p < 0.05$.

3. Results and discussion

3.1. Study area characteristics

The riverine water (RW) had a salinity of 1.5, indicating the occurrence of a small percentage of seawater, and the coastal seawater (SW) had a salinity of 38.5. The temperature was almost the same in the RW (21.2 °C) and in the SW (21.9 °C). Chlorophyll-a showed values higher than 1 mg m^{-3} in the SW, with a maximum (~5 mg·m^{-3}) close to the Arno river mouth (Fig. 1), suggesting that the river input affected phytoplankton distribution up to 15 km from the coast, mainly northward.

The Arno river discharge was highly variable during 2012 (Fig. 2). The average discharge was 1.98 $km^3 \cdot y^{-1}$, with 2 minima in the periods: January–April (0.5 $km^3 \cdot y^{-1}$) and July–September (0.4 $km^3 \cdot y^{-1}$). Higher values were registered in Spring (April–June, 1.8 $km^3 \cdot y^{-1}$) with a maximum between October and the end of December (5.6-40 $km^3 \cdot y^{-1}$). The sampling day was characterized by a discharge of 2.2 $km^3 \cdot y^{-1}$, slightly different from both the average of the year, and the average of October (1.5 $km^3 \cdot y^{-1}$).

3.2. DOM dynamics in RW and SW

3.2.1. DOC concentration

DOC concentration was 365 ± 0.6 μM in RW, and 67 ± 1.0 μM in SW. These values are similar to those reported in previous studies carried out in the same area [14,20,21]. The small discrepancy among these studies can be explained by river discharge and/or the extent of riverine plume. As an example, a stronger riverine influence in SW (lower salinity) can explain the higher seawater DOC concentration reported in the previous studies [20,21].

It is worth noting that DOC concentration is 100–200 μM higher in the Arno river than in the 4 major Mediterranean Sea rivers (Tevere, Po, Ebro and Rhone) (Table 1), despite both the discharge and the length of the Arno river are much lower than those of these major rivers. The high DOC concentration can be attributed to a higher input along its flow (industrial and agricultural waste and/or anthropogenic inputs from the cities).

The published [14,20,21] and unpublished data, collected at the mouth of the Arno river, were merged together in order to study the effect of dilution in DOC distribution at the river mouth (Fig. 3). Taking into consideration the average values DOC shows a conservative

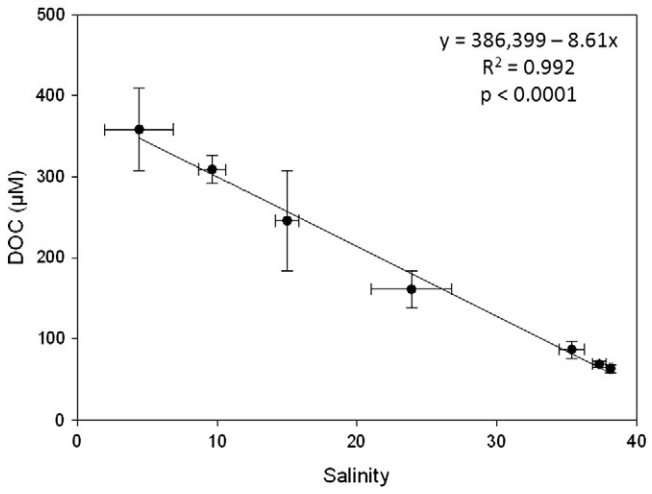

Fig. 3. Mean dissolved organic carbon (DOC) vs. salinity values at the river mouth and in its proximity, error bars refer to the standard deviation.

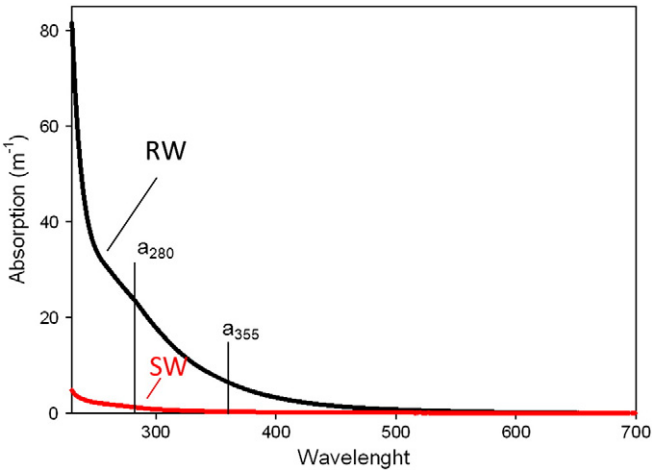

Fig. 4. Absorption spectra of RW (black) and SW (red) samples. Both spectra are the average of the spectra of the three replicates. Absorption coefficient at 280 nm (a_{280}) and 355 nm (a_{355}).

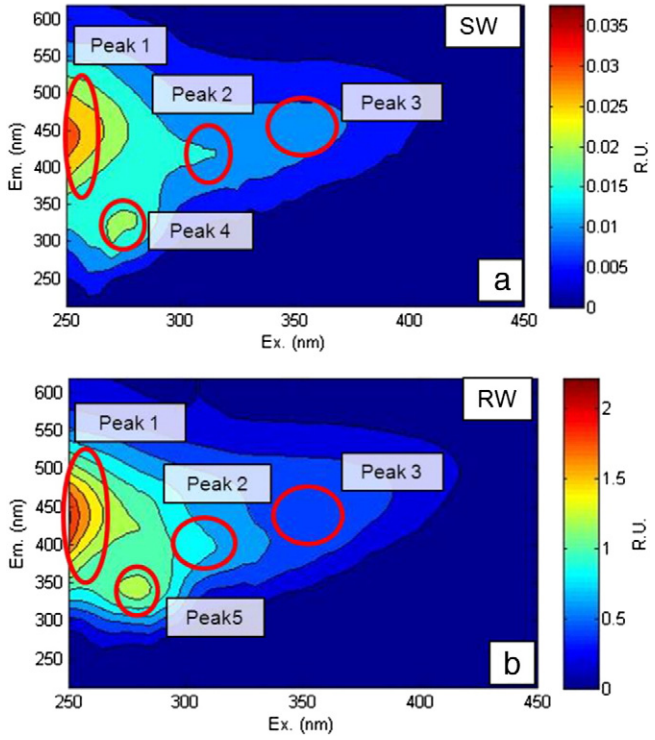

Fig. 5. Average of three replicates Excitation–emission matrixes (EEMs) of SW (a) and RW (b). Note the marked difference in the color scale. R.U.: Raman Units.

behavior. However where there are high standard deviations one can assume that other processes may affect DOC distribution.

In order to have a rough estimate of the total input of DOC by Arno river, the river discharge was multiplied by both the average DOC concentration, that was estimated taking into account the published data (360 μM, Table 1), and the value calculated by using the intercept of the linear relationship between DOC and salinity (386 μM, Fig. 3). This rough calculation indicates that the Arno river may account for 11.23–12.04·10^9 g DOC·y^{-1}, that is 1.7% of the total DOC riverine input to the Mediterranean Sea, though its discharge is just 0.8% (Table 1, [23]). However it is important to take into consideration that samples collected with a high temporal resolution within 1 year would be necessary to make an accurate estimate.

3.2.2. Absorption coefficients and spectral slope

SW and RW absorption spectra showed a similar shape with the typical exponential decay at increasing wavelengths (Fig. 4). In the RW, the absorption coefficients (a_{280} = 24.18 m^{-1} and a_{355} = 7.02 m^{-1}) were markedly higher than in the SW (a_{280} = 1.26 m^{-1} and a_{355} = 0.3 m^{-1}). These values are in agreement with those observed in September 1997 in the same area (a_{280} = 21.6 m^{-1} and a_{355} = 5.18 m^{-1} in the RW and a_{280} = 1.43 m^{-1} and a_{355} = 0.27 m^{-1} in the SW) [20]. A decrease in CDOM absorption was also observed moving from the mouth of the Rhone river (a_{355} = 2.42 m^{-1}) to seawater (a_{355} = 0.09 m^{-1}) [17]. Finally, absorption coefficients in SW were similar to those observed close to the mouth of the Po river (a_{280} = 1.6 m^{-1} and a_{355} = 0.3 m^{-1}) [16]. These results suggest that moving from the river to the sea, CDOM undergoes different biological and physical processes that lead to a decrease in the absorption coefficient.

S was calculated in order to gain indirect information about the molecular characteristics of CDOM. S indicates how fast the absorption decreases with increasing wavelengths and it has been reported to be inversely related to aromatic content and molecular weight of the molecules [13,29,39]. Taking into consideration the values of the spectral slope calculated in different ranges, some interesting similarities can be highlighted. In RW, $S_{275–295}$ showed a value of 0.014 nm^{-1}, similar to that reported for riverine waters in the Gulf of Mexico (0.013 nm^{-1}) [13] while the value in SW (0.025 nm^{-1}) was half of that observed in offshore oligotrophic waters (0.048 nm^{-1}) [13]. Those authors reported that $S_{275–295}$ is correlated with the percentage of terrestrial DOC (tDOC) (their Fig. 7) [13] and according to their results, $S_{275–295}$ values observed in our study suggest the occurrence of 100% of tDOC in RW and ~15% in SW.

Values of $S_{350–400}$ (0.017 ± 8.7 · 10^{-6} nm^{-1} in RW and 0.014 ± 8.6 · 10^{-5} nm^{-1} in SW) were similar to that reported for the Elizabeth river and Chesapeake Bay [29]. In agreement with their observations, $S_{275–295}$ was higher than $S_{350–400}$ in SW, while the opposite was observed in RW. According to these authors, S_R (ratio between $S_{275–295}$ and $S_{350–400}$) was also calculated and it is interesting to observe that for the two rivers the values are similar (0.83 this study, 0.88 Elizabeth river) and they increase in the coastal areas (1.8 this study,

Table 2
Excitation–emission matrix (EEM) peaks. Comparison between peaks found in SW and in RW EEMs with those identified in previous studies.

This study	Coble [40]	Kowalczuk et al. [41]	Para et al., [17]
Peak 1 (SW and RW) Ex 250/Em 400–500 Fulvic-like	**A** Ex 260/Em 380–460 Humic	**C1 + C2** Ex 250/Em 452 Ex 250/Em 420 Terrestrial humic	**A** Ex 260/Em 430–440 UVC humic
Peak 2 (SW) Ex 315/Em 419 **Peak 2 (RW)** Ex 315/Em 400 Marine humic-like	**M** Em 380?420 Marine humic/Em 380–420 Marine humic	**C3** Ex 250(310)/Em 400 Marine and terrestrial humic, possible microbial reprocessing	**M** Ex 300/Em 380–400 Marine humic
Peak 3 (SW) Ex 350/Em 450 **Peak 3 (RW)** Ex 350/Em 420 Humic-like	**C** Ex 350/Em 420–480 Humic	**C4** Ex 270(390)/Em 508 Terrestrial humic substances	**C** Ex 350/Em 430–450 UVA humic
Peak 4 (SW) Ex 270/Em 315 Tyrosine-like	**B** Ex 275/Em 305 Tyrosine	**C5** Ex 270/Em 332 Tyrosine + component of autochthonous DOM	**B** Ex 275/Em 300–310 Tyrosine
Peak 5 (RW) Ex 280/Em 341 Tryptophan-like	**T** Ex 275/340 Tryptophan	**C6** Ex 250(290)/Em 356 Tryptophan + component of autochthonous DOM	**T** Ex 275/Em 330–350 Tryptophan

1.32 Chesapeake Bay), suggesting a decrease in CDOM molecular weight. The difference between the S_R in the two coastal areas can be attributed to a different influence of the river. Values of $S_{350-500}$ were the same (0.017 nm^{-1}) for the Arno and Rhone rivers [17], while they were slightly different in SW (this study: 0.014 nm^{-1}; Rhone river: 0.018 nm^{-1}). Finally, values of S_{270-DL} (0.016 nm^{-1}) were similar to those reported for the same area in September 1997 [20]. The small changes in absorption and spectral slope values suggest that molecular characteristics of riverine CDOM are similar among the different rivers and did not change in the Arno river between 1997 and 2012.

3.2.3. Fluorescence

Fluorescence confirmed the differences in CDOM between RW and SW. A 75% reduction of fluorescence intensity was observed moving from the river (0.5–2.0 R.U.) to the costal station (0.01–0.03 R.U.) (Fig. 5), this result is in agreement with 60–66% reduction of fluorescence intensity observed moving from the Rhone river to the sea [17] and suggests that dilution, removal and transformation processes, affecting DOC at the river mouths, can also strongly affect CDOM dynamics.

The EEMs, measured in both RW and SW, show four main peaks: three in the excitation–emission wavelengths typical of humic-like compounds (peak 1, peak 2 and peak 3), and one in the excitation–emission wavelengths typical of protein-like compounds (peak 4 in SW and peak 5 in RW) (Fig. 5). In order to identify the peaks, their spectroscopic characteristics were compared to those reported in the literature [17,40,41] (Table 2). Peaks 1 and 3 were identified as a signal of terrestrial humic-like fluorescence, in particular the emission maximum of peak 1 at 400–500 nm is similar to that of fulvic acid [42]. Peak 2 was identified as marine humic-like fluorescence, and is mainly attributed to substances reprocessed by microbes [41]. The two protein-like peaks were attributed to tyrosine-like fluorescence (peak 4) and tryptophan-like fluorescence (peak 5), even if we cannot exclude that the peak 5 was due to the occurrence of organic contaminants [43]. It is worth nothing that the humic-like and the fulvic-like peaks showed the same spectroscopic characteristics in the Arno and Rhone rivers, while the protein-like peak was tryptophan-like in the Arno river and tyrosine-like in the Rhone river. Finally the marine humic-like peak was missing in the Rhone river [17]. These results suggest the occurrence of different protein-like substances in the two rivers that can be due to a different input from the land.

3.3. DOC removal and CDOM transformation

Changes in DOC concentration and in CDOM optical properties (absorption and fluorescence) were followed during the mineralization experiment in order to gain information about DOM removal and transformation processes (a summary of all the results is shown in Table 3).

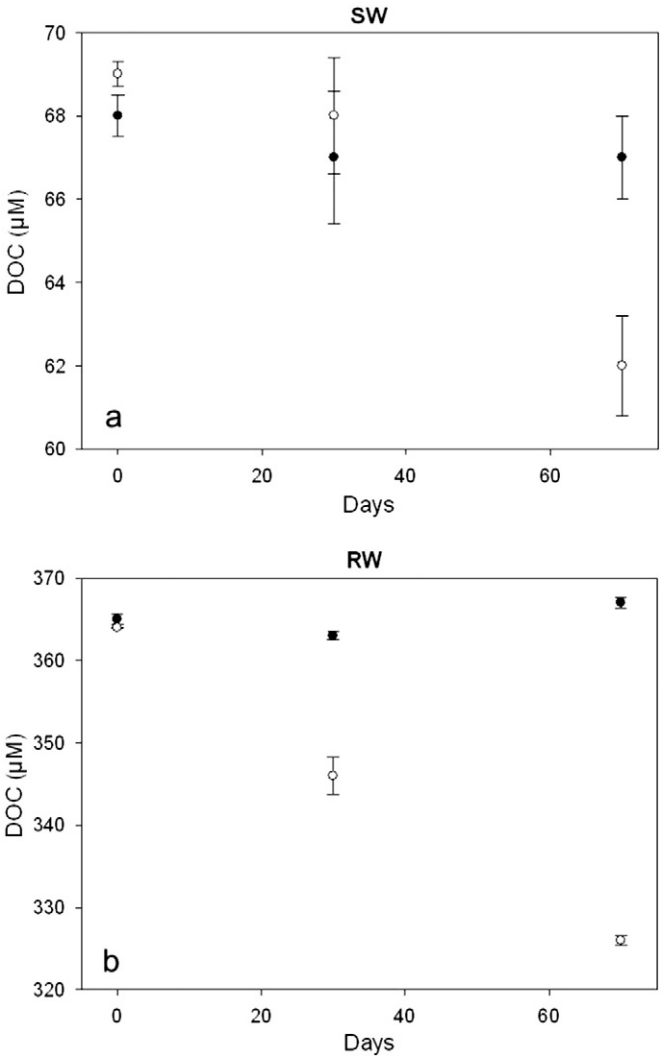

Fig. 6. Dissolved organic carbon (DOC) variation during the experiment in SW (a) and RW (b). Black circles refer to control samples, empty circles refer to mineralized samples. Each point is the average of three replicates, error bars refer to the standard deviation.

3.3.1. DOC

DOC concentration decreased in both RW and SW with time (70 days) (Fig. 6), while no significant variations were observed in the controls. Since the difference between the two treatments was the occurrence of the microbial community in the mineralized sample, the observed changes were attributed to microbial activity.

Table 3
Summary of all measurements made during the mineralization experiment. Values of control samples are not reported since they did not show significant variation. Values reported for mineralized samples are the average ± S.D. of three replicates measured at the different times.

		SW			RW		
Time of experiment (days)		t_0 (0)	t_1 (30)	t_2 (70)	t_0 (0)	t_1 (30)	t_2 (70)
DOC (µM)		67 ± 1.03	68 ± 1.4	62 ± 1.2	365 ± 0.6	346 ± 2.3	326 ± 0.6
a_{280} (m^{-1})		1.26 ± 0.01	1.18 ± 0.009	1.16 ± 0.04	24.18 ± 0.11	22.98 ± 0.04	22.55 ± 0.19
a_{355} (m^{-1})		0.3 ± 0.02	0.26 ± 0.001	0.24 ± 0.02	7.02 ± 0.02	7.01 ± 0.02	6.46 ± 0.05
Protein-like (peak 4/5)	Ex/Em	275/325	275/335	275/318	280/341	280/344	280/344
	F (10^{-2} R.U.)	1.5 ± 0.4	2.6 ± 0.9	2.1 ± 0.02	117 ± 1	132 ± 1	127 ± 2
Fulvic-like (peak 1)	Ex/Em	250/442	250/439	250/436	250/436	250/436	250/436
	F (10^{-2} R.U.)	2.8 ± 0.1	3.7 ± 0.2	3.7 ± 0.07	182 ± 0.9	222 ± 1	215 ± 1
Marine humic-like (peak 2)	Ex/Em	315/419	315/416	315/413	315/400	315/396	316/396
	F (10^{-2} R.U.)	1.4 ± 0.1	1.8 ± 0.1	1.8 ± 0.1	73 ± 0.06	82 ± 0.2	80 ± 0.8
Humic-like (peak 3)	Ex/Em	350/450	350/446	350/446	350/420	350/420	350/423
	F (10^{-2} R.U.)	1.1 ± 0.003	1.4 ± 0.04	1.5 ± 0.04	53 ± 0.04	58 ± 0.04	57 ± 0.5

In RW, DOC decreased from 365 to 346 μM in the first 30 days, and from 346 μM to 326 μM in the following 40 days, suggesting a removal rate of 20 μM DOC·month^{-1} (~0.6 μM DOC·day^{-1}). This value is similar to the DOC removal rates estimated for the northern Adriatic Sea (10–20 μM DOC·month^{-1}) [44].

In SW, DOC showed no significant variations during the first 30 days, while it showed a 6 μM decrease (from 68 μM to 62 μM) between 30th and 70th days, suggesting an average removal rates of 3 μM DOC·month^{-1} (~0.08 μM DOC·day^{-1}), markedly lower than in the river. The lag of 30 days in DOM removal suggests that the DOC, occurring in SW, is not immediately available to the prokaryotic heterotrophs. The same lag was observed by Carlson et al. [45] in a similar incubation experiment carried out with oligotrophic seawater from the Sargasso Sea (initial DOC concentration of 68 μM). This observation can be explained by the molecular characteristics of DOC, making it resistant to rapid microbial utilization, and/or to the inability of the prokaryotic heterotrophs to use the DOC due to its low concentration and/or their low abundance.

The estimated removal rate in SW is three times higher than that reported for the Tyrrhenian Sea (1.1 μM DOC·month^{-1}) [44] and much lower than that observed in a microbial degradation experiment, conducted in a coastal area of Spain, where an exponential decrease of DOC was observed, with a removal rate of ~0.22 μM·day^{-1} [46]. These differences can be attributed to various factors such as: the occurrence of diverse concentrations of semi-labile DOC and/or the capability of microbial communities in the use of bio-available DOC. Similarly, the higher DOC concentration, as well as the occurrence of a higher concentration of semi-labile DOC in the river [19] may explain the faster mineralization rate in RW.

It is interesting to highlight that the same percentage of DOC was removed both in RW (10%) and SW (9%), which suggests that the percentage of semi-labile DOC was similar.

The removed DOC can be used by the heterotrophic prokaryotes to build biomass (net bacterial production) or it can be respired to CO_2 (mineralization). Taking into consideration the values of Bacterial Growth Efficiency (BGE) reported in literature for SW (25%) [47] and RW (4–60%) [48], we can roughly estimate the release of 2.25 μM CO_2 month^{-1} and 6.8–19.2 μM CO_2 month^{-1} in SW and RW, respectively.

3.3.2. Absorption coefficients

In RW, a_{280} showed an exponential decrease with time (Table 3, Fig. 7) and a 6.7% decrease at the end of the experiment (difference between t_0 and t_2 was significant: $p = 0.02$). In contrast, in SW a_{280} showed no significant difference between t_0 and t_2. In RW, a_{355} showed no changes in the first 30 days and a slight decrease during the following 40 days (Table 3, Fig. 7). In SW, a_{355} decreased during the whole experiment (differences between t_0, t_1 and t_2 were significant: $p = 0.02$) with 20% reduction in SW and 8% reduction in RW. The changes in control samples were not significant (RW: $p = 0.9$; SW: $p = 0.2$). We assume that the decrease of absorption is due to the transformation of CDOM by microbial activity.

3.3.3. Fluorescence: EEMs and emission spectra

In order to highlight the changes in fluorescence during the experiment, the EEMs were subtracted by the control and then subtracted one from each other as follows: $t_1 - t_0$ (change in the first month), $t_2 - t_1$ (change in the second month) and $t_2 - t_0$ (change between the beginning and the end of the experiment) (Fig. 8). This representation highlights the increase (positive peaks) or decrease (negative peaks) in fluorescence intensity with time as well as the shift in the position of the peaks.

After the first month, an increase in fluorescence was observed in mineralized samples (Fig. 8a and d). In both SW and RW the $t_1 - t_0$ EEMs showed an increase in the fulvic-like (peak 1), humic-like (peaks 2 and 3) and tryptophan-like peaks (peak 5). An increase in the tyrosine-like fluorescence was only observed in SW (peak 4). A tryptophan-like signal (peak 5) can be observed in SW at t_1, but this peak did not occur in the non-mineralized sample (Fig. 5a), suggesting

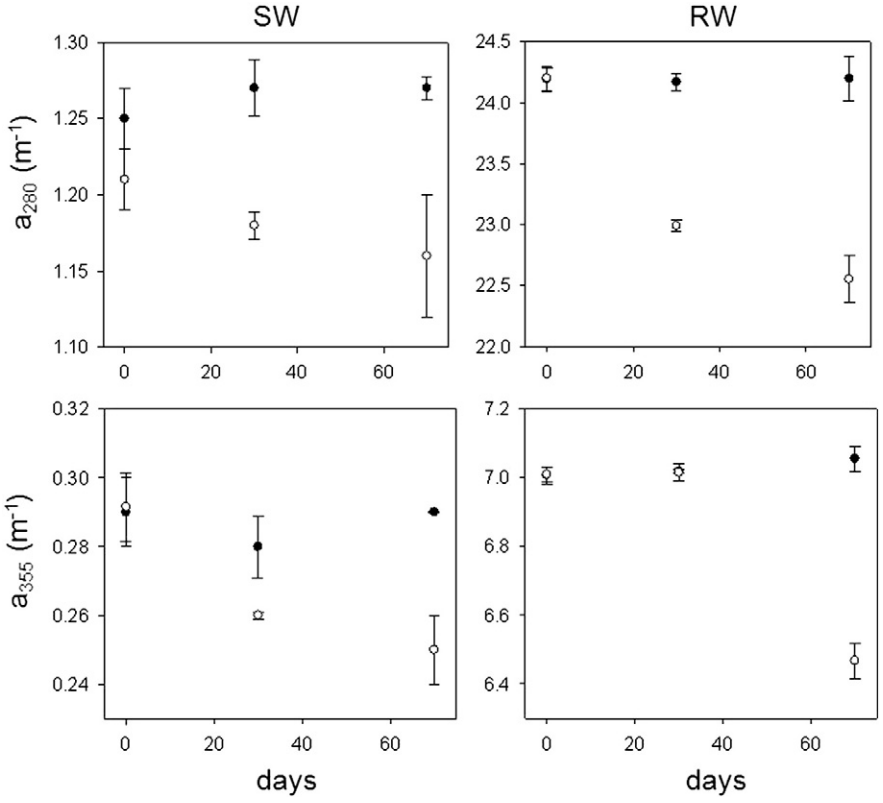

Fig. 7. Absorption coefficient variations during the experiment. Black circles refer to control samples, empty circles refer to mineralized samples. Each point is the average value of three replicates, error bars refer to the standard deviation. Absorption coefficient at 280 nm (a_{280}) and 355 nm (a_{355}).

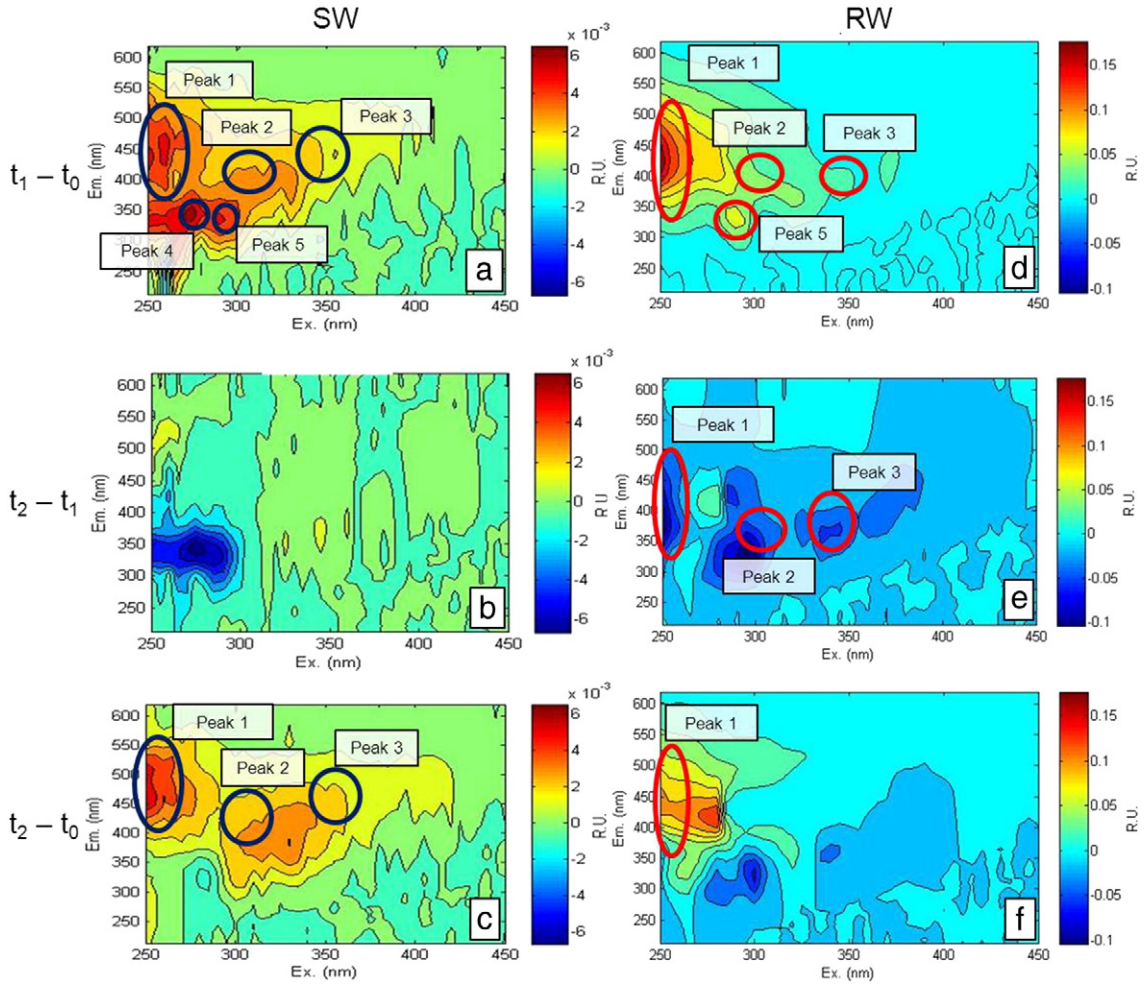

Fig. 8. Differences in fluorescence intensity during the experiment. t_0: start of the experiment, t_1: 30 days, t_2: 70 days. Blue and red circles highlight only the peaks corresponding to significant differences ($p < 0.05$).

that during the experiment molecules containing tryptophan were released.

During the second month ($t_2 - t_1$ EEMs, Fig. 8b and e) most of the fluorescence peaks decreased (negative values). In RW, the fulvic-like, humic-like and marine humic-like peaks (peaks 1, 2 and 3) had negative values suggesting their removal.

Looking at the differences in fluorescence intensities between the beginning and the end of the experiment ($t_2 - t_0$ EEMs, Fig. 8c and f) it is possible to observe that after 70 days (t_2) fulvic-like, humic-like and marine humic-like fluorescence intensities are higher than at t_0.

All the differences in fluorescence intensities reported above were statistically significant ($p < 0.05$) and 10 to 10^3 times higher than the analytical variation.

These results are in agreement with previous studies, which reported an initial release of CDOM by heterotrophic prokaryotes followed by its removal [49–51]. This behavior was attributed to the production of labile CDOM that was consumed on a short temporal scale.

Looking more in detail at the fluorescence spectra, a shift in the emission maxima was observed for almost all peaks (Table 3). The shifts were small (0–4 nm) in RW mineralized sample, while they were 3–10 nm in SW mineralized sample.

These shifts in emission peaks suggest a change in CDOM characteristics during the experiment, since the variation in emission maxima could indicate a change in molecular weight of the chromophores. The intensities of fluorescence peaks (Table 3) highlight higher variability in the SW than RW. After 70 days (t_2) the protein-like signal increased of 8% in RW and of 40% in SW, while the humic-like increased between 7 and 18% in SW and between 28 and 36% in SW.

It is worth noting that absorption coefficients show an exponential decrease with time (Fig. 7, Table 3), while fluorescence increased in the first 30 days and then decreased during the following 40 days (Fig. 8, Table 3). These observations suggest that these chromophores can change their quantum yield due to (i) nonspecific interactions, and (ii) changes in their chemical structure and/or (iii) in the environmental conditions (e.g. pH).

4. Conclusions

The data reported in this study indicate that the Arno river is an important source of DOC and CDOM to the coastal area. Dilution is the main process affecting the distribution of DOM moving from the river to the sea. However, other processes play a role in DOM transformation and removal at the river mouth as highlighted by the mineralization experiment. Our results suggest an important role of the microbial community in DOC removal, with efficiency markedly higher in the river than in the seawater. Biochemical processes may play a crucial role also in the production, removal and transformation of CDOM in both the river and in the seawater.

All the above highlights the complexity of the study system and the importance of fluorescence and absorption spectroscopy as key tools in the understanding of DOM dynamics. This study suggests the need for further studies on the main biophysical processes responsible for DOM

removal and transformation and the application of new spectroscopic tool to answer the many unresolved questions about DOM lability.

Acknowledgments

This research was supported by PERSEUS project, funded by the European Commission under Seventh Framework Program Theme "Oceans of Tomorrow" OCEAN.2011-3, Grant Agreement No. 287600, and by the Italian Flagship project RITMARE funded by the Italian Ministry of Research and University (www.ritmare.it).

The authors wish to thank the Regional Hydrological Service of Tuscany for supplying the Arno river discharge data, and Gianluca Volpe for elaborating the chlorophyll satellite map.

References

[1] D.A. Hansell, Recalcitrant dissolved organic carbon fractions, Ann. Rev. Mar. Sci. 5 (2013) 421–445.
[2] C.L. Sabine, R.A. Feely, N. Gruber, R.M. Key, K. Lee, J.L. Bullister, R. Wanninkhof, C.S. Wong, D.W.R. Wallace, B. Tilbrook, F.J. Millero, T. Peng, A. Kozyr, T. Ono, A.F. Rios, The oceanic sink for anthropogenic CO_2, Science 305 (5682) (2004) 367–371, http://dx.doi.org/10.1126/science.1097403.
[3] P. Amiotte Suchet, J.L. Probst, W. Ludwig, Worldwide distribution of continental rock lithology: implications for the atmospheric/soil CO_2 uptake by continental weathering and alkalinity river transport to the oceans, Glob. Biogeochem. Cycles 17 (2) (2003), http://dx.doi.org/10.1029/2002GB001891.
[4] S.V. Smith, J.T. Hollibaugh, Coastal metabolism and the oceanic organic-carbon balance, Rev. Geophys. 31 (1993) 75–89, http://dx.doi.org/10.1029/92RG02584.
[5] R. Sempéré, B. Charrière, F. Van Wambeke, G. Cauwet, Carbon inputs of the Rhone River to the Mediterranean Sea: biogeochemical implications, Glob. Biogeochem. Cycles 14 (2000) 669–681, http://dx.doi.org/10.1029/1999GB900069.
[6] S.V. Smith, F.T. Mackenize, The ocean as a net heterotrophic system: implication from the carbon biogeochemical cycle, Glob. Biogeochem. Cycles 1 (1987) 187–198, http://dx.doi.org/10.1029/GB001i003p00187.
[7] A. Borges, B. Delille, M. Frankignoulle, Budgeting sinks and sources of CO_2 in the coastal oceans: diversity of ecosystems counts, Geophys. Res. Lett. 32 (2005), http://dx.doi.org/10.1029/2005GL023053.
[8] G. Cauwet, DOM in the coastal zone, in: D.A. Hansell, C.A. Carlson (Eds.), Biogeochemistry of Marine Dissolved Organic Matter, Elsevier, San Diego, 2002, pp. 579–611.
[9] M. Søndergaard, C.A. Stedmon, N.H. Borch, Fate of terrigenous dissolved organic matter (DOM) in estuaries: aggregation and bioavailability, Ophelia 57 (2003) 161–176, http://dx.doi.org/10.1080/00785236.2003.10409512.
[10] K. Mopper, D.J. Kieber, Marine Photochemistry and Its Impacts on Carbon Cycling, Cambridge University Press, Cambridge, U.K., 2000
[11] T.J. Boyd, C.L. Osburn, Changes in CDOM fluorescence from allochthonous and autochthonous sources during tidal mixing and bacterial degradation in two coastal estuaries, Mar. Chem. 89 (2004) 189–210, http://dx.doi.org/10.1016/j.marchem.2004.02.012.
[12] R.S. Poretsky, S. Sun, M. Xiaozhen, M.A. Moran, Transporter genes expressed by coastal bacterioplankton in response to dissolved organic carbon, Environ. Microbiol. 12 (2010) 616–627, http://dx.doi.org/10.1111/j.1462-2920.2009.02102.x.
[13] C.G. Fichot, R. Benner, The spectral slope coefficient of chromophoric dissolved organic matter (S275–295) as a tracer of terrigenous dissolved organic carbon in river-influenced ocean margins, Limnol. Oceanogr. 57 (5) (2012) 1453, http://dx.doi.org/10.4319/lo.2012.57.5.1453.
[14] S. Vignudelli, C. Santinelli, R. Murru, L. Nannicini, A. Seritti, Distributions of dissolved organic carbon (DOC) and chromophoric dissolved organic matter (CDOM) in Coastal waters of the northern Tyrrhenian Sea (Italy), Estuar. Coast. Shelf Sci. 60 (2004) 133–149, http://dx.doi.org/10.1016/j.ecss.2003.11.023.
[15] A.I. Gómez-Gutiérrez, E. Jover, L. Bodineau, J. Albaigés, J.M. Bayona, Organic contaminant loads into the Western Mediterranean Sea: estimate of Ebro River inputs, Chemosphere 65 (2006) 224–236, http://dx.doi.org/10.1016/j.chemosphere.2006.02.058.
[16] D. Berto, M. Giani, F. Sacelli, E. Centenni, C.R. Ferrari, B. Pavoni, Winter to spring variations of chromophoric dissolved organic matter in a temperate estuary (Po River, northern Adriatic Sea), Mar. Environ. Res. 70 (2010) 73–81, http://dx.doi.org/10.1016/j.marenvres.2010.03.005.
[17] J. Para, P.G. Coble, B. Charrière, M. Tedetti, C. Fontana, R. Sempéré, Fluorescence and absorption properties of chromophoric dissolved organic matter (CDOM) in a Coastal surface waters of the northwestern Mediterranean Sea, influence of the Rhône River, Biogeosciences 7 (2010) 4083–4103, http://dx.doi.org/10.5194/bgd-7-5675-2010.
[18] G.M. Ferrari, The relationship between chromophoric dissolved organic matter and dissolved organic carbon in the European Atlantic coastal area and in the West Mediterranean Sea (Gulf of Lions), Mar. Chem. 70 (4) (2000) 339–357.
[19] C. Panagiotopoulos, R. Sempéré, J. Para, P. Raimbault, C. Rabouille, B. Charrière, The composition and flux of particulate and dissolved carbohydrates from the Rhone River into the Mediterranean Sea, Biogeosciences 9 (5) (2012) 1827–1844.
[20] A. Seritti, D. Russo, L. Nannicini, R. Del Vecchio, DOC, absorption and fluorescence properties of estuarine and coastal waters of the Northern Tyrrhenian Sea, Chem. Speciat. Bioavailab. 10 (1998) 95–106.
[21] M. Gonnelli, S. Vestri, C. Santinelli, Chromophoric dissolved organic matter and microbial enzymatic activity. A biophysical approach to understand the marine carbon cycle, Biophys. Chem. 182 (2013) 79–85.
[22] M. Pettine, L. Patrolecco, M. Camusso, S. Crescenzio, Transport of carbon and nitrogen to the Northern Adriatic Sea by the Po River, Estuar. Coast. Shelf Sci. 46 (1998) 127–142, http://dx.doi.org/10.1006/ecss.1997.0303.
[23] C. Santinelli, DOC in the Mediterranean Sea, in: D.A. Hansell, C.A. Carlson (Eds.), Biogeochemistry of Marine Dissolved Organic Matter, Academic Press, Elsevier, Burlington, 2015, pp. 579–608.
[24] R. Santoleri, G. Volpe, S. Marullo, B. Buongiorno Nardelli, Open waters optical remote sensing of the Mediterranean Sea, in: Vittorio Barale, Martin Gade (Eds.), Remote Sensing of the European Seas, 2008, pp. 103–116.
[25] D.A. Hansell, Dissolved organic carbon reference material program, EOS Trans. Am. Geophys. Union 86 (35) (2005) 318.
[26] C. Thomas, G. Cauwet, J.F. Minster, Dissolved organic-carbon in the equatorial Atlantic-Ocean, Mar. Chem. 49 (2–3) (1995) 155–169, http://dx.doi.org/10.1016/0304-4203(94)00061-H.
[27] C. Santinelli, L. Nannicini, A. Seritti, DOC dynamics in the meso and bathypelagic layers of the Mediterranean Sea, Deep-Sea Res. II Top. Stud. Oceanogr. 57 (16) (2010) 1446–1459.
[28] A.A. Andrew, R. Del Vecchio, A. Subramaniam, N.V. Blough, Chromophoric dissolved organic matter (CDOM) in the Equatorial Atlantic Ocean: optical properties and their relation to CDOM structure and source, Mar. Chem. 148 (2012) 33–43.
[29] J.R. Helms, A. Stubbins, J.D. Ritchie, E.C. Minor, D.J. Kieber, K. Mopper, Absorption spectral slopes and slope ratios as indicators of molecular weight, source, and photobleaching of chromophoric dissolved organic matter, Limnol. Oceanogr. 53 (3) (2008) 955–969.
[30] C.A. Stedmon, R. Bro, Characterizing dissolved organic matter fluorescence with parallel factor analysis: a tutorial, Limnol. Oceanogr. Methods 6 (2008) 572–579.
[31] J.R. Lakowicz, Principles of Fluorescence Spectroscopy, Springer, 2009.
[32] R.E. Carlson, F.N. Fritsch, An algorithm for monotone piecewise bicubic interpolation, SIAM J. Numer. Anal. 26 (1) (1989) 230–238, http://dx.doi.org/10.1137/0726013.
[33] A.J. Lawaetz, C.A. Stedmon, Fluorescence intensity calibration using the Raman scatter peak of water, Appl. Spectrosc. 63 (8) (2009) 936–940.
[34] E. Sherr, B. Sherr, Understanding roles of microbes in marine pelagic food webs: a brief history, in: D.L. Kirchman (Ed.), Microbial Ecology of the Oceans, Wiley, 2008, pp. 27–44.
[35] M. Troussellier, H. Schäfer, N. Batailler, L. Bernard, C. Courties, P. Lebaron, G. Muyzer, P. Servais, J. Vives-Rego, Bacterial activity and genetic richness along an estuarine gradient (Rhone River plume, France), Aquat. Microb. Ecol. 28 (2002) 13–24.
[36] M. Celussi, A. Paoli, Aubry F. Bernardi, M. Bastianini, P. Del Negro, Diel microbial variations at a coastal Northern Adriatic station affected by Po river outflows, Estuar. Coast. Shelf Sci. 76 (2008) 36–44.
[37] R.R. Sokal, F.J. Rohlf, Biometry: The Principles and Practice of Statistics in Biological Research, 3rd ed. WH Freeman and Company, San Francisco, CA, USA, 1995.
[38] W. Ludwig, E. Dumont, M. Meybeck, S. Heussner, River discharges of water and nutrients to the Mediterranean and Black Sea: major drivers for ecosystem changes during past and future decades? Prog. Oceanogr. 80 (3) (2009) 199–217.
[39] N.V. Blough, S.A. Green, Spectroscopic characterization and remote sensing of non-living organic matter, in: R.G. Zepp, C. Sonntag (Eds.), The Role of Non-living Organic Matter in the Earth's Carbon Cycle, Wiley, Chichester, 1995, pp. 23–45, http://dx.doi.org/10.1016/S0304-4203(02)00036-1.
[40] P.G. Coble, Characterization of marine and terrestrial DOM in seawater using excitation–emission matrix spectroscopy, Mar. Chem. 51 (1996) 325–346, http://dx.doi.org/10.1016/0304-4203(95)00062-3.
[41] P. Kowalczuk, M.J. Durako, H. Young, A.E. Kahn, W.J. Cooper, M. Gonsior, Characterization of dissolved organic matter fluorescence in the South Atlantic Bight with use of PARAFAC model: interannual variability, Mar. Chem. 113 (2009) 182–196, http://dx.doi.org/10.1016/j.marchem.2009.01.015.
[42] C.A. Stedmon, S. Markager, Resolving the variability in dissolved organic matter fluorescence in a temperate estuary and its catchment using PARAFAC analysis, Limnol. Oceanogr. 50 (2) (2005) 686–697.
[43] A. Baker, Fluorescence excitation–emission matrix characterization of some sewage-impacted rivers, Environ. Sci. Technol. 35 (2001) 948–953.
[44] C. Santinelli, D.A. Hansell, M. Ribera d'Alcalà, Influence of stratification on marine dissolved organic carbon (DOC) dynamics: the Mediterranean Sea case, Prog. Oceanogr. 119 (2013) 68–77.
[45] C.A. Carlson, S.J. Giovannoni, D.A. Hansell, S.J. Goldberg, R. Parsons, K. Vergin, Interactions among dissolved organic carbon, microbial processes, and community structure in the mesopelagic zone of the northwestern Sargasso Sea, Limnol. Oceanogr. 49 (4) (2004) 1073–1083.
[46] C. Lønborg, X.A. Álvarez-Salgado, K. Davidson, S. Martínez-García, E. Teira, Assessing the microbial bioavailability and degradation rate constants of dissolved organic matter by fluorescence spectroscopy in the coastal upwelling system of the Ría de Vigo, Mar. Chem. 119 (2010) 121–129, http://dx.doi.org/10.1016/j.marchem.2010.02.001.
[47] P.A. Del Giorgio, J.J. Cole, Bacterial energetics and growth efficiency, in: D.L. Kirchman (Ed.), Microbial Ecology of the Oceans, Wiley, 2000, pp. 289–325.
[48] F. Roland, J.J. Cole, Regulation of bacterial growth efficiency in a large turbid estuary, Aquat. Microb. Ecol. 20 (1999) 31–38.
[49] N.B. Nelson, D.A. Siegel, A.F. Michaels, Seasonal dynamics of colored dissolved material in the Sargasso Sea, Deep-Sea Res. I Oceanogr. Res. Pap. 45 (6) (1998) 931–957.
[50] N.B. Nelson, D.A. Siegel, Chromophoric DOM in the Open Ocean, in: D.A. Hansell, C.A. Carlson (Eds.), Biogeochemistry of Marine Dissolved Organic Matter, Elsevier, San Diego, 2002, pp. 547–578, http://dx.doi.org/10.1016/j.dsr.2007.02.006.
[51] N.B. Nelson, C.A. Carlson, D.K. Steinberg, Production of chromophoric dissolved organic matter by Sargasso Sea microbes, Mar. Chem. 89 (2004) 273–287, http://dx.doi.org/10.1016/j.marchem.2004.02.017.